metals

MDPI

Article

Numerical and Experimental Investigation of the Influence of Growth Restriction on Grain Size in Binary Cu Alloys

Andreas Cziegler [1,*], Olga Geraseva [2] and Peter Schumacher [1,3]

1 Department Metallurgy, Chair of Casting Research, Montanuniversitaet Leoben, Franz-Josef-Straße 18, A-8700 Leoben, Austria; peter.schumacher@unileoben.ac.at
2 Materials Center Leoben Forschung GmbH, Roseggerstraße 12, A-8700 Leoben, Austria; olga.geraseva@mcl.at
3 Austrian Foundry Research Institute, Parkstraße 21, A-8700 Leoben, Austria
* Correspondence: andreas.cziegler@unileoben.ac.at; Tel.: +43-3842-402-3303

Received: 2 September 2017; Accepted: 18 September 2017; Published: 20 September 2017

Abstract: Grain refinement by elemental addition has been extensively investigated within the last decades in Al or Mg alloys. In contrast, in the Cu system, the role of solute on grain size is less investigated. In this study, the grain refinement potency of several alloying elements of the Cu system was examined. To predict grain size depending on the growth restriction factor Q, grain size modelling was performed. The results obtained by the grain size model were compared to variations in the grain size of binary Cu alloys with increasing solute content under defined cooling conditions of the TP-1 grain refiner test of the Aluminium Association©. It was found that the experimental results differed significantly from the predicted grain size values for several alloying elements. A decreasing grain size with increasing alloy concentration was observed independently of the growth restriction potency of the alloying elements. Furthermore, excessive grain coarsening was found for several solutes beyond a transition point. It is assumed that contradictory variations in grain size result from a change in the nucleating particle density of the melt. Significant decreases in grain size are supposed to be due to the in-situ formation of potent nucleation sites. Excessive grain coarsening with increasing solute content may occur due to the removal of nucleating particles. The model shows that the difference in the actual number of particles before and beyond the transition point must be in the range of several orders of magnitude.

Keywords: cast; metallurgy; Cu alloy; growth restriction; grain refinement

1. Introduction

In alloy castings, fine and equiaxed grains are desirable [1], resulting in improved mechanical properties, a reduction of defects such as microporosity, and furthermore in an improved castability [2], e.g., in an improved feeding behaviour resulting in a reduced likelihood of hot tearing. The final grain size of an alloy casting is dependent on the casting process; more precisely, on the cooling rate ($\dot{T}$), the solute content, and the amount of inoculating particles [3], either via the addition of master alloys or by in situ formation. Grain refinement by inoculation has been extensively investigated for several decades [4], mainly in the field of Al alloys, both helping to understand the mechanism of grain refinement and to develop efficient master alloys, where the Al-Ti-B system is nowadays mainly used [5]. The ideas developed in the field of Al alloys have been successfully transferred to other alloy systems, such as Mg alloys [6].

Compared to Al and Mg alloys, Cu alloys are less often investigated in the field of grain refinement [7]. Studies that have been carried out within the last decades [8–17] that are of an empirical

nature reveal that the grain refinement of Cu-based alloys seems to be strongly dependent on the alloy system, the solute contents, trace elements and impurities, and furthermore on the casting conditions. Due to the different alloy systems under investigation, the addition of several alloying elements, and varying casting conditions, there is still a lack of a detailed fundamental investigation in the field of Cu alloys to understand their grain refinement mechanism.

A recent study of in situ-generated oxide and boride particles under defined cooling conditions given by the TP-1 grain refiner test [18] was carried out by Balart et al. [19]. However, it was found that the grain refinement of pure Cu by particle inoculation via in situ-generated particles reveals some difficulties. The effect of nanoparticles on the grain size of Cu-based alloys has been recently studied by Chen et al. [20–22]. Fe-rich nanoparticles with diameters less than 100 nm that precipitate from the liquid at high cooling rates are supposed to be potent nucleants for Cu, while this is in contrast to the free-growth theory proposed by Greer et al. [3], and are assumed to restrict growth that opens new fields of research with regard to grain refiners that resist poisoning [23]. However, several questions have to be answered to quantify the effect of nanoparticles on grain refinement.

As it is well-accepted in the literature [24] that grain refinement depends not only on nucleation, but also on growth restriction by segregating solutes, there is a need for a sophisticated investigation of the growth restriction effect of alloying elements in the Cu system. The parameter that describes the effect of alloying elements on grain size is known as the growth restriction factor (Q) that is given by Equation (1) [25,26]:

$$Q = m(k-1)c_0, \quad (1)$$

where m is the slope of the liquidus line, k is the partition coefficient, and c_0 is the solute concentration. The higher the Q value, the finer the grain size due to a slower growth rate, a slower latent heat release, and a higher undercooling for more particles to become active [27]. The first empirically determined values of a type of growth restriction factor in Cu alloys were given by Northcott [28] by investigation of the growth restriction of columnar grains under unidirectional cooling at small alloying additions. Subsequently, with the introduction of supercooling by Tiller et al. [29], this growth restriction factor would correspond to the supercooling parameter P that is Q/k, where k is the partition coefficient.

However, Q-values for several alloying elements of the Cu system using binary phase diagrams were first given by Cziegler and Schumacher [30]. Nevertheless, the evaluation of Q via binary phase diagrams is strongly dependent on the resolution of the respective phase diagram, and is therefore proposed to be used as a rough approximation only. A more accurate and comprehensive list of Q-values was given by Balart et al. [31] using calculated binary phase diagrams evaluated by thermodynamic software tools. Recently, accurately determined Q-values by cooling calculations using thermodynamic software tools were given by Cziegler and Schumacher [32].

As it was found for Al alloys [3] and Mg alloys [6] that decreasing grain size correlates with increasing Q, the objective of this study was to investigate the correlation between Q and grain size in Cu alloys both experimentally under defined cooling conditions given by the TP-1 grain refiner test and by grain size modelling based on Greer's [3] free-growth model.

2. Materials and Methods

2.1. Melt Treatment Procedure

Based on given Q-values [32], nine alloying elements with various growth restriction potency were investigated in the experiments in addition to unalloyed reference samples. A set of Cu-based alloys with single additions of Mg, S, P, Te, Ti, Zr, Ni, Cr, and Bi in the range of up to approximately 1 wt % was prepared using commercially pure Cu (99.9 wt %) as base material. The chemical analysis of the base material is given in Table 1. The chemical analysis of the binary Cu-based alloys is shown in Table 2. The chemical analysis was performed by spark analysis (OBLF VeOS©). In each case, 2100 g of the base material was remelted to 1250 $\pm$ 5 °C in a clay-graphite crucible in an induction furnace.

Table 1. Chemical analysis of commercially pure Cu used as base material in this work.

Element (wt %)							
Sn	Pb	Zn	Ni	P	S	Bi	Cr
<0.0005	<0.0005	0.0332	<0.001	<0.001	<0.001	<0.002	<0.0005
Mg	Te	Ti	Zr	Si	Fe	Al	Cu
<0.0001	<0.001	<0.0004	<0.0003	<0.001	<0.0005	<0.0003	balance

Table 2. Data of *Q* and alloy concentration (main alloying element) of TP-1 samples cooled after transfer to the water-quench.

Alloy System (Alloy No.)	Solute Concentration (wt %)	*Q* (K)	Alloy System (Alloy No.)	Solute Concentration (wt %)	*Q* (K)
Cu-Mg (1)	0.002	0.06	Cu-Ti (6)	0.708	6.16
Cu-Mg (2)	0.007	0.19	Cu-Ti (7)	1.627	14.15
Cu-Mg (3)	0.023	0.67	Cu-Zr (1)	0.001	0.01
Cu-Mg (4)	0.066	1.93	Cu-Zr (2)	0.012	0.10
Cu-Mg (5)	0.185	5.43	Cu-Zr (3)	0.023	0.19
Cu-Mg (6)	0.346	10.08	Cu-Zr (4)	0.091	0.76
Cu-S (1)	0.051	1.44	Cu-Zr (5)	0.182	1.52
Cu-S (2)	0.092	2.60	Cu-Zr (6)	0.398	3.33
Cu-S (3)	0.219	6.20	Cu-Zr (7)	0.814	6.82
Cu-S (4)	0.373	10.55	Cu-Ni (1)	0.011	0.04
Cu-S (5)	0.583	16.49	Cu-Ni (2)	0.06	0.21
Cu-P (1)	0.012	0.32	Cu-Ni (3)	0.12	0.42
Cu-P (2)	0.043	1.16	Cu-Ni (4)	0.241	0.85
Cu-P (3)	0.087	2.35	Cu-Ni (5)	0.381	1.34
Cu-P (4)	0.189	5.11	Cu-Ni (6)	0.564	1.94
Cu-P (5)	0.298	8.05	Cu-Ni (7)	0.949	3.35
Cu-P (6)	0.501	13.54	Cu-Bi (1)	0.009	0.02
Cu-P (7)	0.958	25.89	Cu-Bi (2)	0.036	0.13
Cu-Te (1)	0.001	0.01	Cu-Bi (3)	0.098	0.35
Cu-Te (2)	0.013	0.17	Cu-Bi (4)	0.176	0.62
Cu-Te (3)	0.062	0.81	Cu-Bi (5)	0.248	0.88
Cu-Te (4)	0.175	2.29	Cu-Bi (6)	0.449	1.58
Cu-Te (5)	0.299	3.91	Cu-Bi (7)	0.897	3.17
Cu-Te (6)	0.564	7.38	Cu-Cr (1)	0.001	0.003
Cu-Te (7)	1.225	16.02	Cu-Cr (2)	0.013	0.04
Cu-Ti (1)	0.001	0.01	Cu-Cr (3)	0.049	0.17
Cu-Ti (2)	0.014	0.12	Cu-Cr (4)	0.113	0.39
Cu-Ti (3)	0.058	0.51	Cu-Cr (5)	0.226	0.78
Cu-Ti (4)	0.197	1.72	Cu-Cr (6)	0.389	1.34
Cu-Ti (5)	0.375	3.26	Cu-Cr (7)	0.786	2.71

During the melting step, the crucibles were covered with a graphite brick, sealed with fibrous material, and the melting occurred under Ar atmosphere to avoid the oxidation of the melt. After charging the base material and sealing the crucible, the pure Cu was remelted at 1250 ± 5 °C and held for 1 min before adding stoichiometrically calculated P as CuP15 for deoxidation due to a residual O-content of approximately 200 ppm in the base material. After the addition of CuP15, the melt was held for 1 min for deoxdiation before alloying was performed using commercially pure Cu-50Mg, Cu-20S, Cu-15P, Cu-50Zr, Cu-28Ti, Cu-50Te, and Cu-10Cr master alloys and commercially pure Ni and Bi. After the alloying step, the melt was held for 5 min at 1250 ± 5 °C. Consecutively, the melt was poured into a preheated (316 °C) graphite-coated TP-1 mould, followed by a rapid transfer to the TP-1 water-quench, where the mould was left for 5 min. For the melting step, both the alloying and holding of the melt was under Ar atmosphere, whereas the pouring was performed in air. The TP-1 test was operated at a water temperature of approximately 10 °C and a flow rate in accordance with the TP-1 test procedure [18].

The samples were sectioned horizontally at a height of 39 mm from the bottom surface, ground, and polished to a height of 38 mm to avoid a recrystallization structure. A standard metallographic procedure was applied to the samples and etched to reveal the microstructure. The majority of the samples were etched using a mixture of 10.5 g Fe(III)Cl + 2.5 mL HCl (25%) to 100 mL ethanol. Samples with higher P-content were etched with a mixture of 100 mL copper ammonium chloride + 10 mL NH_3 (25%). Samples with higher Bi- and S-content were etched with a mixture of 10 g ammonium persulfate to 100 mL H_2O. The grain size was determined on the base of the intercept method as per ASTM: E112-13 by counting the number of grain-boundary intercepts along the horizontal and vertical lines of five areas in the centre of the sample in agreement with the TP-1 test procedure [18].

As $\dot{T}$ is used as an input parameter in the grain size model, $\dot{T}$ before the onset of freezing was determined using a type K thermocouple mounted at a height of 38 mm from the bottom surface of the TP-1 mould in the centre of the mould using pure Cu (99.9 wt %) as reference material. The cooling curve was determined with a frequency of 4 s^{-1}. Due to thermal fluctuations, the precise nucleation temperature could not be measured. Therefore, $\dot{T}$ before the onset of freezing [33] was defined as the local $\dot{T}$ close to the solidification temperature of pure Cu at 1085 °C. For the sample solidified in the water-quench, a $\dot{T}$ of approximately 4 $K{\cdot}s^{-1}$ was evaluated.

2.2. Model Description

To predict the variation of grain size depending on the alloy concentration, respectively, growth restriction factor Q grain size modelling has been performed based on Greer's [3] free-growth model, as it provides a numerical model to quantitatively predict grain size dependent on Q. The accuracy of the model was tested in Al alloys [3], and the results of the model agreed with measured grain sizes given in the work of Spittle and Sadli [34]. Furthermore, the model was successfully transferred to the Mg system, as shown by Günther et al. [35].

2.2.1. Grain Initiation

As specified by Kurz and Fisher [36], equiaxed grain growth can only occur in an undercooled melt. This undercooled melt can be assumed to be spatially isothermal, as suggested by Maxwell and Hellawell [37], due to the higher magnitude of the thermal diffusion coefficient compared to the solute diffusion coefficient. In the numerical model of Maxwell and Hellawell [37], the nucleation and growth of spherical grains on a set of particles with equal diameter is assumed. The latent heat evolved by the growth of spherical grains causes the melt temperature to rise above the heterogeneous nucleation temperature, suppressing further nucleation events. Due to the growth restriction potency of alloying elements, there is a restriction on growth and latent heat release that allows time for further nucleation events to occur.

The limitation of a single particle size was overcome by the development of the free-growth model by the group of Greer et al. [3]. In the numerical model based on Maxwell and Hellawell's [37] isothermal melt model, grain initiation is assumed to occur in an isothermal melt, in which a distribution of particles is predefined by an added refiner. The particles are treated as discs with a diameter d. A nucleus that is formed on the face of the particle as a spherical cap can grow laterally across the face, but further growth outward from the particle is limited by the Gibbs-Thomson effect [3,38]. Further growth of the nucleus is possible only by reducing the radius of curvature of its interface with the melt. In the case that the radius of curvature is greater than the critical radius r^*, depending on undercooling, grain initiation is not possible. The critical radius r^* is given by [36]:

$$r* = 2\sigma/\Delta S_v \Delta T, \quad (2)$$

where σ is the solid/liquid interfacial energy, and ΔS_v is the entropy of fusion per volume unit. Growth of the nucleus becomes possible only by decreasing r^* if the undercooling is increased. Free growth of

nuclei on these particles can therefore occur only if the undercooling required for grain initiation is reached, that is, ΔT_{fg}. The relationship between ΔT_{fg} and d is given by [3]:

$$\Delta T_{fg} = 4\sigma/\Delta S_v d. \quad (3)$$

The nucleation and growth of grain is initiated on the biggest particles first. With increasing undercooling, progressively further smaller particles become activated and act as nucleation sites. This continues until recalescence hinders the activation of further particles.

2.2.2. Grain Growth

In an isothermal melt below the liquidus temperature (T_l), the radius r of a growing grain at time t is given by [3]:

$$r = \lambda\sqrt{D_s t}, \quad (4)$$

where D_s is the solute diffusion coefficient, and λ is the invariant-size approximation [3]:

$$\lambda = \left(-S/2\sqrt{\pi}\right) + \sqrt{(S^2/4\pi - S)}, \quad (5)$$

where S can be given by [39]:

$$S = -2(\Delta T - \Delta T_c)/Q, \quad (6)$$

where ΔT is the total undercooling, and ΔT_c is the curvature undercooling. Thermal undercooling and kinetic undercooling are neglected in the model, and only ΔT_c and the solute undercooling ΔT_s are significant. ΔT_c can be given by [3]:

$$\Delta T_c = 2\sigma/\Delta S_v r. \quad (7)$$

The growth rate of a spherical crystal V can be derived by the differentiation of Equation (4) with respect to time [3]:

$$V = dr/dt = \lambda_s^2 D_s/2r. \quad (8)$$

2.2.3. Calculation of Solidified Grain Size

The numerical calculations were performed for a volume element of 1 m^3. Binary alloys with the composition given in Table 2 were assumed to cool down from T_l with a constant $\dot{T}$. Above the critical undercooling of the largest particles, the evolution of the melt temperature can be calculated by [3]:

$$T_{n+1} = T_n - \dot{T}dt, \quad (9)$$

where dt is the time step, T_n is the melt temperature in the nth time interval and T_{n+1} is the temperature in the $(n + 1)$th time interval. As soon as the melt undercooling reaches the critical undercooling of the largest particle, nucleation and growth of grains is initiated of a set of particles with radius r in the range $r + dr$, whereas the number of particles in that range is $N(r)dr$. The heat input $q(r)dr$ of the growing crystals on the set of particles with radius r to $r + dr$ in the nth time interval is given by [3]:

$$q(r)dr = N(r)dr \cdot \frac{4\pi}{3} \cdot r_{n-1}^2 \cdot (r_n - r_{n-1}) \cdot \Delta H_v, \quad (10)$$

where ΔH_v is the latent heat of fusion per volume unit, whereas in all subsequent time intervals the radius r of the crystal increases according to [3]:

$$r_{n+1} = r_n - Vdt, \quad (11)$$

with V calculated in the nth time interval taking r of the $(n-1)$th time interval. The evolution of the melt temperature can then be evaluated by [3]:

$$T_{n+1} = T_n - \dot{T}\mathrm{d}t + q_{\mathrm{tot}}/c_{\mathrm{pv}}, \tag{12}$$

where q_{tot} is the heat input of all growing crystals in the nth to $(n+1)$th time interval, and c_{pv} is the specific heat per unit volume.

The number of activated particles was summed up until recalescence occurs, and the final grain size was calculated by Equation (13) [3]:

$$N_{\mathrm{v}} = \frac{0.5}{l^3}, \tag{13}$$

where N_{v} is the number of grains per unit volume, and l is the grain size determined by the linear intercept method.

The model [3] was implemented in Matlab©R2015a for further processing using a time step dt of 10^{-3} s. For each test series of binary alloys, the particle size distribution was assumed to be given by an exponential function [38]:

$$N(r) = \frac{N_0}{r_0}\exp(-r/r_0), \tag{14}$$

where $N(r)$ is the number of particles in the range r to r + dr, N_0 is the total number of particles in the melt and r_0 is the characteristic radius. The average grain size of the unalloyed reference samples was determined to be 688.90 µm and 669.68 µm, respectively. Assuming a cube-root relationship between the number of activated particles and grain size measurement that is given by Equation (13), the number of activated particles is in the range of approximately 1.6×10^9 m^{-3}. Considering that the number of activated particles is at least two orders of magnitude lower than the total amount of particles in the melt [38], a particle density of 1.6×10^{11} m^{-3} can be assumed. In the calculation, the total number of particles N_0 was defined to be 10^{12} m^{-3}. The particle diameter was assumed to be in the range 10 µm to 0.1 µm with a particle diameter step of 0.01 µm in the calculation, whereas the characteristic d was assumed arbitrary to be 0.4 µm to facilitate stable calculation conditions. The solute diffusion coefficient in the melt D_{Fe} [40] of Fe was defined to be constant for all alloying elements under investigation. Further physical data used for the calculations are given in Table 3. From the chemical composition given in Table 1, it can be derived that Zn is the dominant solute with the main impact on growth restriction. Therefore, commercially pure Cu with a nominal Zn concentration of 0.0332 wt % (Q = 0.0332 K) was used as base material for grain size modelling. The impact on growth restriction of the alloying elements was added to 0.0332 K.

Table 3. Physical data used for calculations.

Parameter	Symbol	Value	Ref.
Solid/liquid interfacial energy	γ	0.177 J·m^{-2}	[41]
Entropy of fusion	ΔS_{v}	1.2×10^6 J·m^{-3}·K^{-1}	[36]
Enthalpy of fusion	ΔH_{v}	1.62×10^9 J·m^{-3}	[36]
Heat capacity of melt	c_{pv}	3.96×10^6 J·m^{-3}·K	[36]
Diffusivity of solute in melt	D_{Fe}	3.88×10^{-9} m^2·s^{-1}	[40]

3. Results and Discussion

3.1. Grain Size Modelling

Figure 1 depicts the predicted relationship between grain size and alloy concentration for the alloying elements under investigation (S and Bi are not included in the figure). Grain size is plotted

against the nominal alloy concentration in the range 0–1 wt %. From this concept, the impact on grain size of the alloying elements with various growth restriction potency should be derived. Considering only the impact of growth restriction on grain size with the assumption of a constant particle size distribution and density, disregarding any further interaction of the alloying elements with impurities, the variation in grain size with increasing alloy concentration is expected as shown in Figure 1. For the parameters used in the calculation, the range between 100 µm and 150 µm was determined as the saturation level beyond that grain size does not change significantly. Elements with high growth restriction potency, Mg, P, S are expected to reduce grain size significantly at low alloy concentrations. The saturation level is reached in the range of approximately 0.1 wt %, whereas alloying elements with low *Q*-values, Ni, Bi, Cr are expected to refine the microstructure to a minor degree. The saturation level is predicted to be reached in the range of 0.5 wt %. The capability of the calculation is limited by the fact that no master alloy with a known particle size distribution was added to the melt. This is also related to the lack of accessible commercial grain refiners for Cu alloys. Furthermore, a constant diffusion coefficient was used in the model and the influence of the solute diffusion zone on the nucleation potency of inoculating particles known as solute suppressed nucleation given by Shu et al. [27] was neglected.

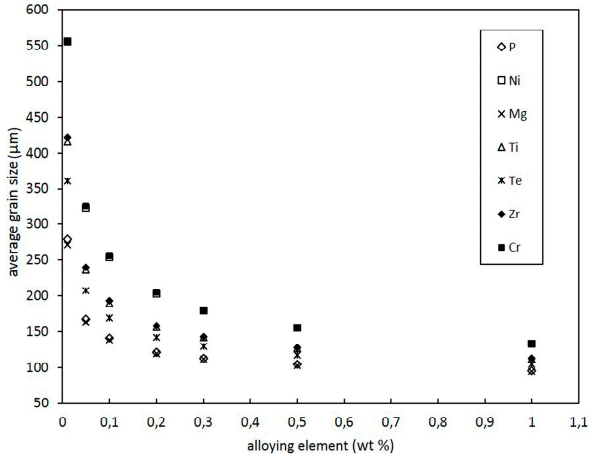

Figure 1. Predicted grain size vs. concentration for the alloying elements under investigation. S and Bi are not included in the figure.

3.2. Effect of Alloying Elements and Concentration on Grain Size of Binary Cu Alloys

A comprehensive experimental study on the influence of alloying elements and their concentration on the grain size of binary Al alloys, both without and with added grain refiner, was carried out by Spittle and Sadli [34]. The results presented in the work provide perspective on the correlation between decreasing grain and increasing solute content, both for binary samples with and without grain refiner added. Furthermore, a saturation of grain size was observed at higher solute contents, as grain size remains rather constant above a critical alloy level. Greer et al. [3] and Shu et al. [27] used the experimental data provided by Spittle and Sadli [34] for comparison with their prediction models showing the correlation between grain size and *Q* of binary Al alloys. A similar correlation of *Q* and grain size in binary Mg alloys was reported by Lee et al. [42].

In contrast, the influence of solute content and *Q* on the grain size of binary Cu alloys is less investigated and remains outstanding. The empirical work carried out by Bustos [17] shows the influence of 0.1 wt % of various alloying elements on the grain size of pure Cu. However, only limited data is given for increasing alloy concentration. Furthermore, grain size was observed to increase for several alloying elements at 0.1 wt %, and no comparison with a valid supercooling parameter (*P*) or *Q* were given, as *Q*-values for Cu alloys have just been recently reported [30–32]. This raises the question:

can a similar correlation be found for Q and grain size in Cu alloys as has been observed for Al and Mg alloys?

To overcome the complexity of the influence of various casting conditions on the grain size, the TP-1 grain refiner test of the Aluminium Association© [18] was adapted in this work for Cu. However, due to the melting and casting process used in this work, the test procedure of the Aluminium Association© [18] had to be modified. The melt was poured in the air into the TP-1 ladle instead of plunging the ladle into the melt for 30 s. Therefore, the chill effects of the mould despite preheating and convection effects have to be considered, which may have influenced the results obtained in this work. Nevertheless, as the TP-1 test has been successfully used in other alloy systems, e.g., Mg alloys [43], it offers a foundation for future work in the field of grain refinement of Cu alloys, in particular with regard to the development and investigation of the efficiency of grain refiners, and it has been used successfully by Balart et al. [19].

Figures 2–4 show the grain size data obtained by the melting experiments and the results obtained by grain size modelling, where grain size is plotted vs. the alloy concentration. One can see that grain size decreases with increasing alloy concentration for several alloying elements, as expected. Figures 5–7 show representative macrographs of the TP-1 samples, sectioned in a height of 38 mm from the bottom surface of the samples. The diameter of the samples is 45 mm. Macrographs of the samples reveal a columnar microstructure at the other area of the specimens. This may be due to the adapted TP-1 process, as the melt was poured into the ladles instead of plunging the ladle into the melt.

Mg is the element with the highest Q-factor of the alloying elements under investigation, and is expected to reduce grain size significantly with increasing alloy concentration and Q-value. The effect of Mg additions on the grain size of Cu is shown in Figure 2a. The addition of small amounts of Mg (<0.1 wt %) slightly reduces grain size. However, a remarkable increase in grain size can be observed beyond a transition point. When increasing Mg content to approximately 0.35 wt %, excessive grain coarsening occurs that differs severely from the correlation between grain size and alloy concentration in Al [3,34] or Mg alloys [6,42]. In contrast, S, as an element with an equal Q-value (28.29 K/wt % [32]) compared to Mg (29.33 K/wt % [32]), significantly reduces grain size, as shown in Figure 2c. A low level of grain size can be found even at low alloy concentrations of approximately 0.05 wt %. Beyond 0.2 wt % S, grain size slightly increases. However, it remains rather constant at a low level. Compared to the data obtained by grain size modelling, grain size was predicted to be lower than observed in the experiments under the conditions of the TP-1 grain refiner test. As already mentioned, the modelling ability is limited by the fact that no commercial grain refiner with a known particle distribution was added to the melt. Furthermore, a constant diffusion coefficient was used for the alloys under investigation, and the effect of solute-suppressed nucleation, as shown by Shu et al. [27], was not considered in the model. As P (Q = 27.03 K/wt % [32]) is a commonly used alloying element for deoxidation in Cu alloys, it is of interest to determine its effect on grain size. From Figure 2b, one can see that the predicted grain size differs significantly from the grain size determined in the experiments. Furthermore, it was found that the initial grain size at low P contents is higher than for the unalloyed reference samples. With increasing additions of P, the grain size becomes smaller, but tends to increase beyond a transition point of approximately 0.1 wt % P.

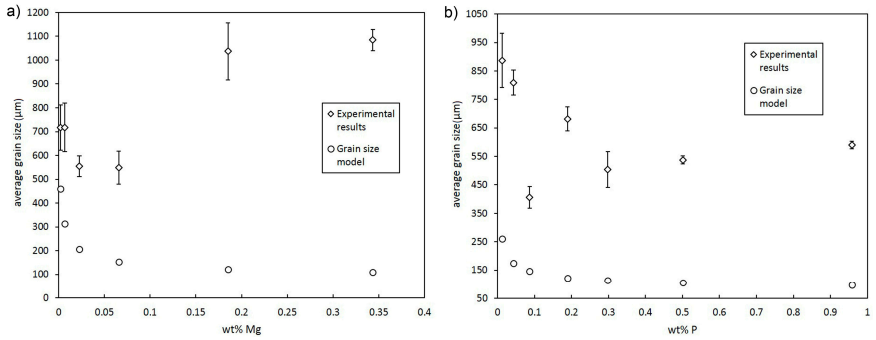

Figure 2. *Cont.*

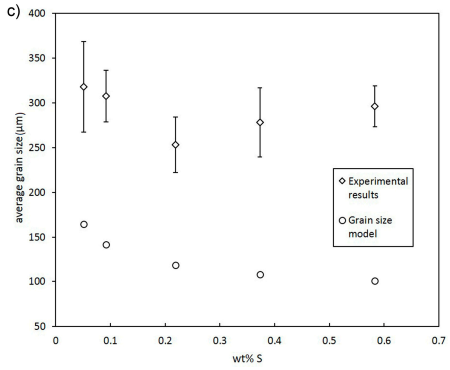

Figure 2. Grain size as a function of Mg (**a**), P (**b**) and S (**c**).

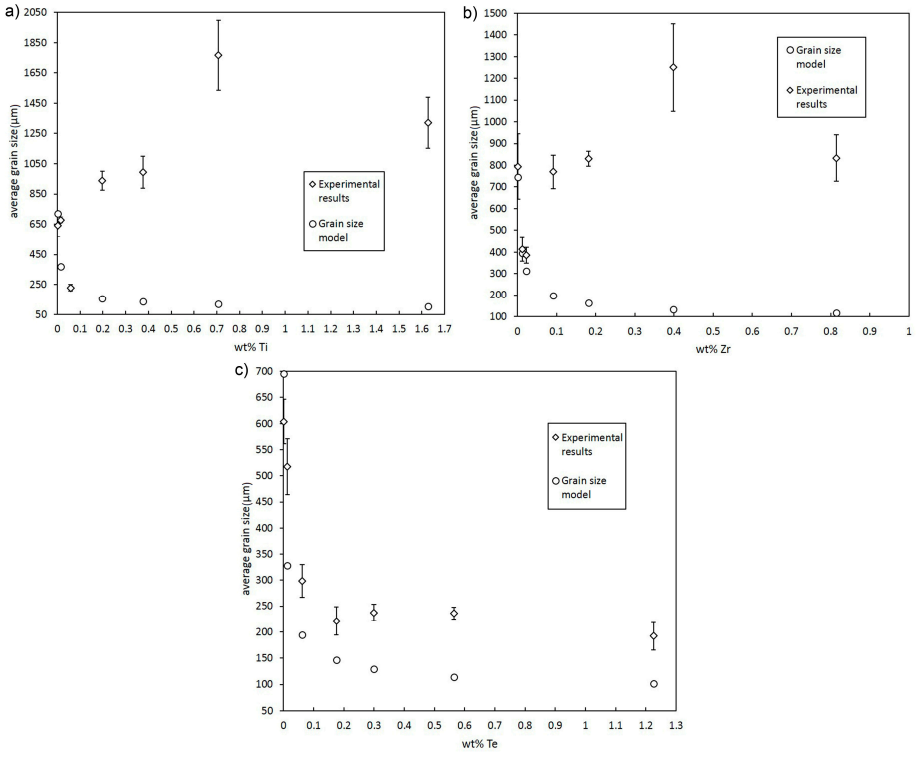

Figure 3. Grain size of Cu with various levels of Ti (**a**), Zr (**b**) and Te (**c**).

In contrast to Mg, S, and P, Te has a slightly smaller *Q*-factor (13.08 K/wt % [44]). Nevertheless, Te remarkably decreases grain size to very low levels, as indicated in Figure 3c. Furthermore,

the predicted grain size is in good agreement with the values obtained in the melting experiments. Te concentrations up to approximately 0.2 wt % significantly reduce grain size to a saturation level at about 200 µm. Higher additions of Te do not show any further significant grain refinement. From Figure 3a,b, it can be clearly seen that the alloying elements Ti and Zr show results similar in trend compared to Mg. Low alloy concentrations of both Ti and Zr efficiently decrease grain size to low levels. However, excessive grain coarsening can be observed beyond a transition point. The predicted grain size is in good agreement with the measured grain size at low alloy concentrations, but differs severely beyond the transition point.

The opposite was found for alloying elements with a low *Q*-factor, Ni (Q = 3.53 [32]) and Bi (Q = 3.53 [32]), shown in Figure 4a,b. Despite low *Q*-values and therefore expected low growth restriction potency, grain size significantly decreases with increasing alloy concentration to approximately 200 µm. However, a saturation level as found for Te cannot be observed. Compared with this, Cr, as an element with an equal *Q*-factor (3.45 K/wt % [32]) to that of Ni and Bi, shows the opposite (Figure 4c). A similar trend in grain size with increasing alloy concentration compared to Mg, Ti, and Zr was found, as excessive grain coarsening occurs.

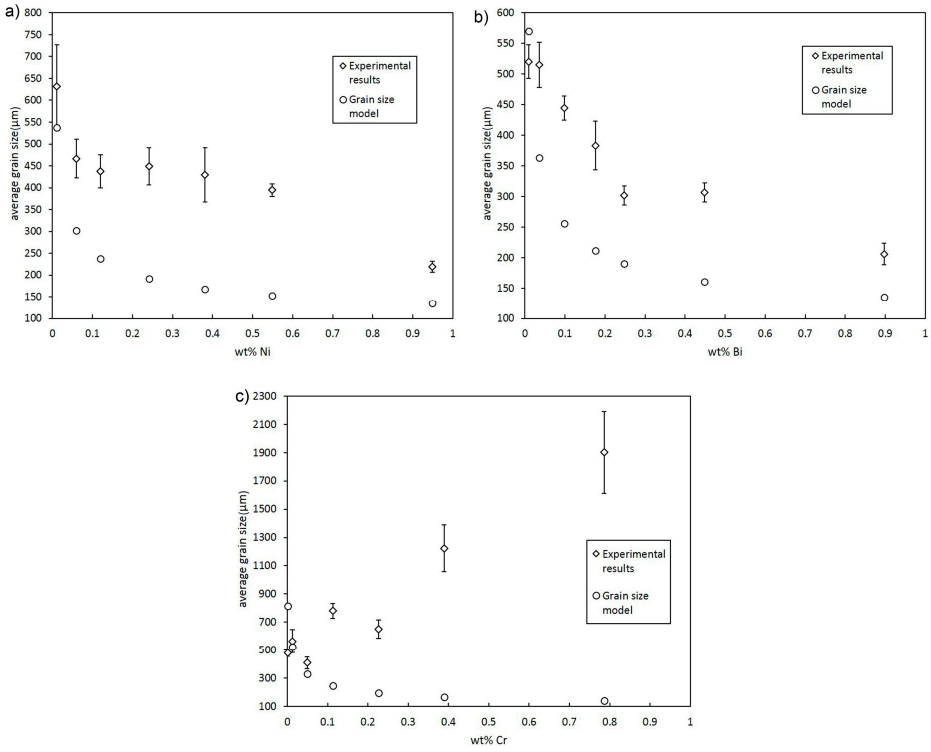

Figure 4. Grain size of Cu with a range of Ni (**a**), Bi (**b**) and Cr (**c**) concentrations.

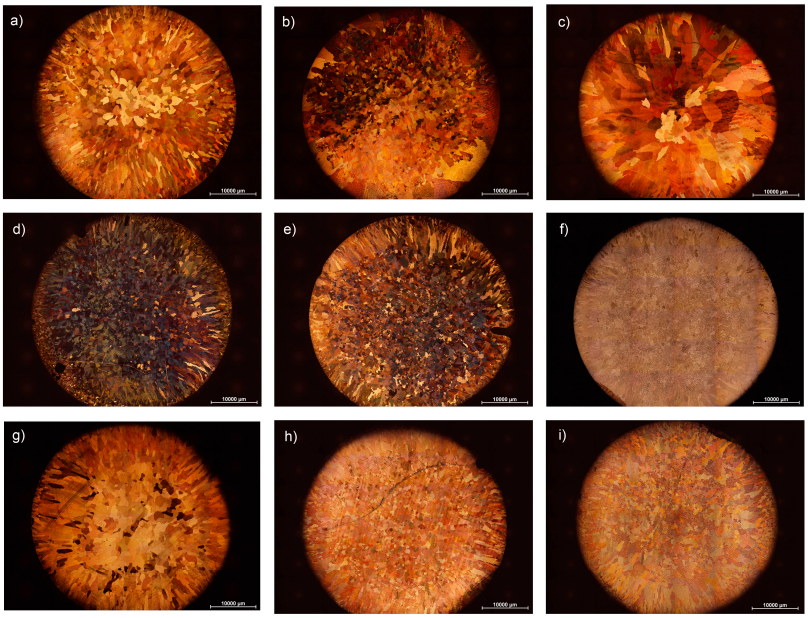

Figure 5. Macrographs of TP-1 samples, sectioned at a height of 38 mm. (**a**) 0.002 wt % Mg, (**b**) 0.023 wt % Mg, (**c**) 0.346 wt % Mg, (**d**) 0.051 wt % S, (**e**) 0.092 wt % S, (**f**) 0.373 wt % S, (**g**) 0.012 wt % P, (**h**) 0.087 wt % P, and (**i**) 0.501 wt % P. Macrographs (h) and (i) are reprinted with permission from [32], Taylor and Francis Ltd., 2017.

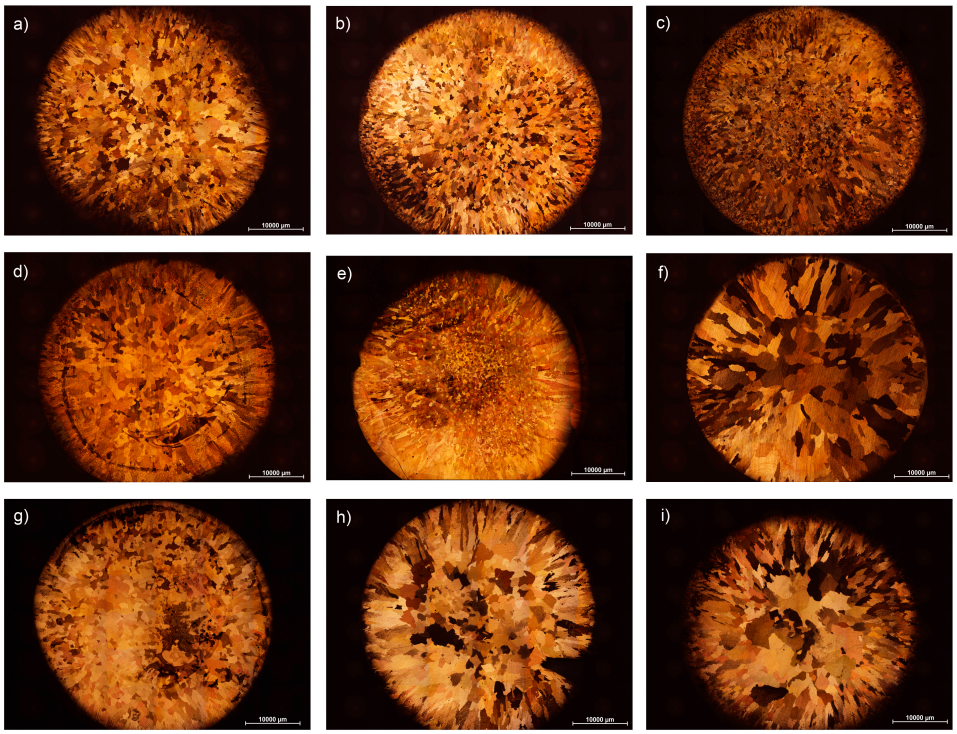

Figure 6. Macrographs of Cu–Te, Cu–Ti and Cu–Zr TP-1 samples. (**a**) 0.001 wt % Te, (**b**) 0.013 wt % Te, (**c**) 0.564 wt % Te, (**d**) 0.014 wt % Ti, (**e**) 0.058 wt % Ti, (**f**) 0.708 wt % Ti, (**g**) 0.012 wt % Zr, (**h**) 0.182 wt % Zr, and (**i**) 0.398 wt % Zr. Macrographs (g) and (i) are reprinted with permission from [32], Taylor and Francis Ltd., 2017.

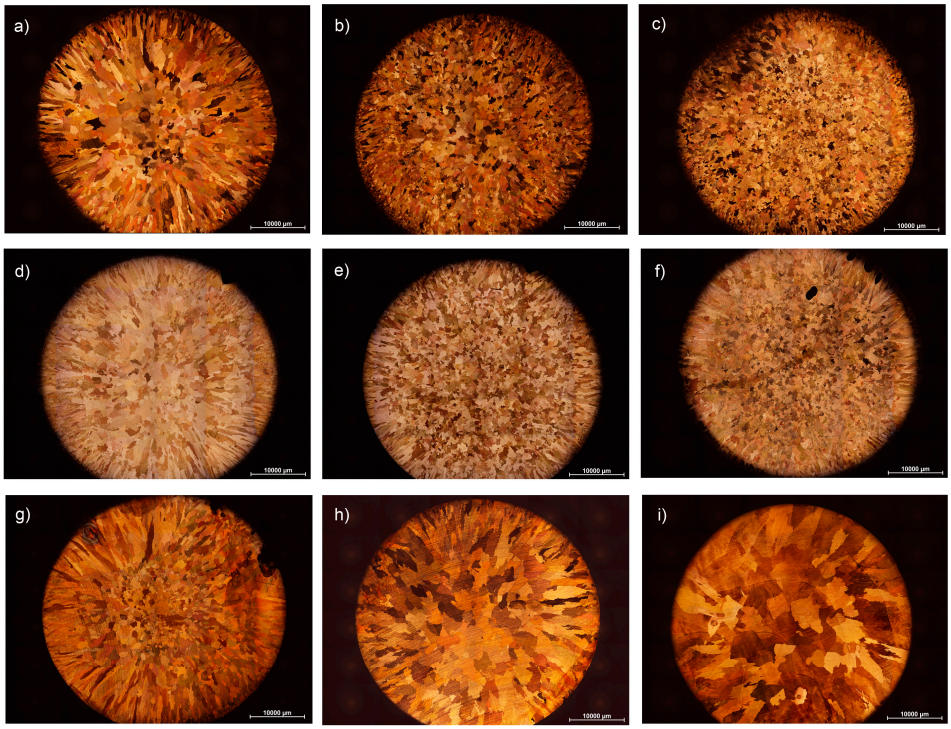

Figure 7. Macrographs of Cu–Ni, Cu–Bi and Cu–Cr alloys. (**a**) 0.011 wt % Ni, (**b**) 0.241 wt % Ni, (**c**) 0.949 wt % Ni, (**d**) 0.036 wt % Bi, (**e**) 0.176 wt % Bi, (**f**) 0.248 wt % Bi, (**g**) 0.001 wt % Cr, (**h**) 0.389 wt % Cr, and (**i**) 0.786 wt % Cr. Macrographs (b) and (c) are reprinted with permission from [32], Taylor and Francis Ltd., 2017.

3.3. Transition in Grain Size in Cu Alloys

When the results of the TP-1 melting experiments are compared with those obtained by grain size modelling, it is clearly observed in Figures 2–4 that grain size shows a transition for several alloying elements that differs severely from the correlation between grain size and Q found for Al [3,34] and Mg alloys [6,42]. Figure 8, where grain size is plotted against Q, depicts the low correlation between Q and grain size in Cu alloys for the alloying elements studied in this work. From the concept of Q, a similar grain size is expected at the same Q-value that is independent of the alloying element. Considering the results obtained in the current work and in the literature [17,30,32], the effect of alloying elements within the concept of growth restriction has to be considered differently compared to Al alloys, which exhibit a stable particle distribution. It should be specified that similar grain sizes at the same Q-value for different alloying elements can only be expected in the case that the particle density is the same [42]. Significant variations in grain size, as found for Mg, P, Ti, Zr, and Cr, could be generated by reactions that may occur by the addition of those alloying elements with potential nucleating particles in the initial melt. In this sense, the formation of non-metallic inclusions and intermetallic compounds by the addition of the alloying elements may contribute to the low correlation between Q and grain size.

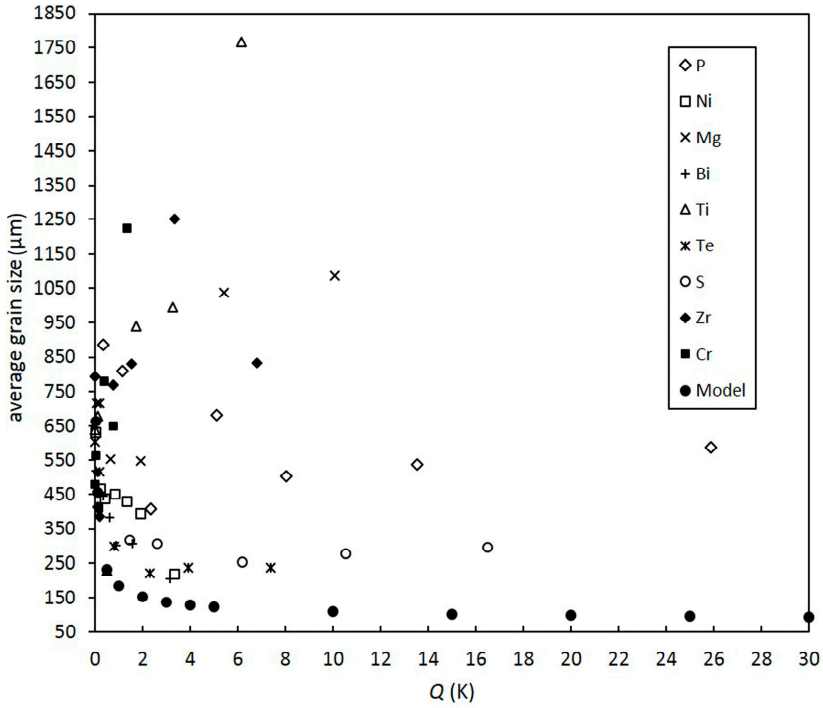

Figure 8. Grain size vs. Q for the alloying elements under investigation and the grain size obtained by the grain size model.

P is an alloying element with a relatively high Q-factor compared to other alloying elements tested in this study, e.g., Bi and Ni. Despite that, the observed grain size is larger. The higher grain size value of the low-alloyed P samples compared to the unalloyed reference samples indicates an interaction between P and potential nucleation sites in the Cu melt. In this sense, it can be assumed that P tends to remove potential nucleating particles as it is a strong deoxidation reagent. In contrast, Ti and Zr, each with a slightly lower Q-factor compared to P, significantly decrease grain size at low alloy concentrations despite the low Q-value. In this context, the formation of potent nucleation sites by the addition of these alloying elements can be assumed via in situ reactions with impurities, potentially residual O, e.g., TiO_2 with a low lattice disregistry to the Cu lattice [44]. The excessive grain coarsening beyond a certain alloy level can be again associated with the removal of particles, potentially via deoxidation reactions, as Zr, Ti, Cr, and Mg are strong deoxidation reagents. Considering a Cu-Ti alloy with a Ti concentration of 0.2 wt %, in which excessive grain coarsening occurs, the grain size observed is in the range of approximately 940 µm compared to approximately 230 µm at an alloy level of 0.06 wt % Ti, as shown in Figure 3a. Assuming a constant particle size distribution in the model, the nucleating particle density has to be decreased to 10^9 m^{-3} compared to the 10^{12} m^{-3} used in the original calculation to reach a grain size level of approximately 900 µm at a Ti concentration of approximately 0.2 wt %. When considering the results obtained in this work for Mg, P, Ti, Zr, and Cr, the difference in the actual number of particles before and beyond the transition points must be in the range of several orders of magnitude. It would be of interest to investigate these aspects further, to determine potential nucleating particle in the initial melt and after the addition of several alloying elements.

4. Conclusions

1. A grain size model based on Greer's free-growth model [3] was used in this work to predict grain size for Cu alloys depending on the growth restriction factor Q.

2. Nine alloying elements with various *Q*-factors were investigated to determine the variation in grain size with increasing solute content under defined cooling conditions of the TP-1 grain refiner test.
3. Despite a low growth restriction potency, Ni, Bi, and Te were found to decrease grain size continuously with increasing alloy concentration. The results obtained by the melting experiments are in good agreement with the results of the grain size model.
4. In addition to Ni, Bi, and Te, S was found to decrease grain size efficiently.
5. Contradictory results were found for Mg, P, Ti, Zr, and Cr, as grain size decreases at low alloy concentrations. However, excessive grain coarsening can be observed with increasing solute content.
6. It is assumed that variations in grain size, as found for Mg, P, Ti, Zr, and Cr, result from a change in the nucleating particle density of the melt that may occur due to reactions of the added alloying elements with particles in the initial melt. Significant decreases in grain size, as found for Ti and Zr, are supposed to be due to the in situ formation of potent nucleation sites, potentially with residual O. Excessive grain coarsening with increasing solute content may occur due to the removal of nucleating particles. The model shows that the difference in the actual number of particles before and beyond the transition point must be in the range of several orders of magnitude.

Acknowledgments: The support of the Austrian Research Promotion Agency (FFG) (No. 845877) is gratefully acknowledged. Thanks to Dipl.-Ing. Thomas Angerer (Montanuniversitaet Leoben, Austria) for his advice during the melting experiments and to Dipl.-Ing. Martin Fechter (Austrian Foundry Research Institute, ÖGI, Austria) for performing the chemical analysis.

Author Contributions: Andreas Cziegler and Peter Schumacher conceived and designed the experiments; Andreas Cziegler performed the experiments; Andreas Cziegler and Olga Geraseva analyzed the data; Andreas Cziegler wrote the paper.

Conflicts of Interest: The authors declare no conflict of interest.

References

1. Easton, M.; StJohn, D. Grain refinement of aluminum alloys: Part I. The nucleant and solute paradigms—A review of the literature. *Metall. Mater. Trans. A* **1999**, *30*, 1613–1623. [CrossRef]
2. Quested, T.E.; Dinsdale, A.; Greer, A.L. Thermodynamic modelling of growth-restriction effects in aluminium alloys. *Acta Mater.* **2005**, *53*, 1323–1334. [CrossRef]
3. Greer, A.L.; Bunn, A.M.; Tronche, A.; Evans, P.V.; Bristow, D.J. Modelling of inoculation of metallic melts: Application to grain refinement of aluminium by Al-Ti-B. *Acta Mater.* **2000**, *48*, 2823–2835. [CrossRef]
4. Murty, B.S.; Kori, S.A.; Chakraborty, M. Grain refinement of aluminium and its alloys by heterogeneous nucleation and alloying. *Int. Mater. Rev.* **2002**, *47*, 3–29. [CrossRef]
5. Quested, T.E. Understanding mechanisms of grain refinement of aluminium alloys by inoculation. *Mater. Sci. Technol.* **2004**, *20*, 1357–1369. [CrossRef]
6. StJohn, D.H.; Qian, M.; Easton, M.A.; Cao, P.; Hildebrand, Z. Grain refinement of magnesium alloys. *Metall. Mater. Trans. A* **2005**, *36*, 1669–1679. [CrossRef]
7. Campbell, J. Casting alloys. In *Complete Casting Handbook*, 1st ed.; Elsevier: Oxford, UK, 2011; pp. 255–390.
8. Cibula, A. Grain-refining additions for cast copper alloys. *J. Inst. Met.* **1954**, *82*, 513–524.
9. Dennison, J.P.; Tull, E.V. The refinement of cast grain-size in copper-aluminium alloys containing 7–9 per cent Aluminium. *J. Inst. Met.* **1957**, *85*, 8–10.
10. Henke, R. Kornfeinung von NE-Metallgußlegierungen. *Gießerei-Praxis* **1965**, *1*, 14–20. (In German)
11. Couture, A.; Edwards, J.O. Kornfeinung von Kupfer-Sandgußlegierungen und ihr Einfluß auf die Güteeigenschaften. *Gießerei-Praxis* **1974**, *21*, 425–435. (In German)
12. Romankiewicz, F.; Ellerbrok, R.; Engler, S. Einfluß einer Kornfeinung mit Zirconium auf Erstarrungsmorphologie, Speisungsvermögen und Festigkeitseigenschaften von Messing CuZn30 und Siliciummessing CuZn15Si4. *Gießereiforschung* **1974**, *39*, 25–33. (In German)

13. Mannheim, R.; Reif, W.; Weber, G. Untersuchung der Kornfeinung von Kupfer-Zinn-Legierungen mit Zirconium und/oder Bor und Eisen sowie ihres Einflusses auf die mechanischen Eigenschaften. *Gießereiforschung* **1988**, *40*, 1–16. (In German)
14. Reif, W.; Weber, G. A New grain refiner for copper-zinc alloys containing 25–42% Zinc. *Metall* **1987**, *41*, 1131–1137.
15. Romankiewicz, F.; Glazowska, I.; Rybakowski, M. Kornfeinung von Kupferlegierungen. *Metall* **1994**, *48*, 865–871. (In German)
16. Sadayappan, M.; Thomson, J.P.; Elboujdaini, M.; Gu, G.P.; Sahoo, M. Grain Refinement of Permanent Mold Cast Copper Base Alloys. Final Report. Available online: https://www.osti.gov/scitech/biblio/823242/ (accessed on 8 July 2017).
17. Bustos, O.C. Untersuchung zur Kornfeinung von Reinst-Kupfer durch Chemische Zusätze und Deutung der Vorgänge. Ph.D. Thesis, TU Berlin, Berlin, Germany, 1990. (In German)
18. The Aluminium Association. *Standard Test Procedure for Aluminium Alloy Grain Refiners: TP-1*; The Aluminium Association: Washington, DC, USA, 2012.
19. Balart, M.J.; Patel, J.B.; Fan, Z. Grain refinement of DHP copper by particle inoculation. *Int. J. Cast Met. Res.* **2015**, *28*, 242–247. [CrossRef]
20. Chen, X.; Wang, Z.; Ding, D.; Tang, H.; Qiu, L.; Luo, X.; Shi, G. Strengthening and toughening strategies for tin bronze alloy through fabricating in-situ nanostructured grains. *Mater. Des.* **2015**, *66*, 60–66. [CrossRef]
21. Chen, K.; Chen, X.; Ding, D.; Shi, G.; Wang, Z. Heterogeneous nucleation effect of in situ iron-rich nanoparticles on grain refinement of copper alloy. *Mater. Lett.* **2016**, *168*, 188–191. [CrossRef]
22. Chen, K.; Chen, X.; Ding, D.; Shi, G.; Wang, Z. Formation mechanism of in-situ nanostructured grain in cast Cu-10Sn-2Zn-1.5Fe-0.5Co (wt %) alloy. *Mater. Des.* **2016**, *94*, 338–344. [CrossRef]
23. Greer, A.L. Overview: Application of heterogeneous nucleation in grain-refining of metals. *J. Chem. Phys.* **2016**, *145*, 211704. [CrossRef] [PubMed]
24. Greer, A.L.; Cooper, P.S.; Meredith, M.W.; Schneider, W.; Schumacher, P.; Spittle, J.A.; Tronche, A. Grain Refinement of Aluminium Alloys by Inoculation. *Adv. Eng. Mater.* **2003**, *5*, 81–91. [CrossRef]
25. Easton, M.A.; StJohn, D.H. A model of grain refinement incorporating alloy constitution and potency of heterogeneous nucleant particles. *Acta Mater.* **2001**, *49*, 1867–1878. [CrossRef]
26. Moriceau, J. Discussion of the mechanisms of aluminum grain refining by titanium and boron. *Rev. L'aluminium* **1972**, *413*, 977–988.
27. Shu, D.; Sun, B.; Mi, J.; Grant, P.S. A quantitative study of solute diffusion field effects on heterogeneous nucleation and the grain size of alloys. *Acta Mater.* **2011**, *59*, 2135–2144. [CrossRef]
28. Northcott, L. The influence of alloying elements on the crystallization of copper: Part I. Small additions and the effect of atomic structure. *J. Inst. Met.* **1938**, *62*, 101–136.
29. Tiller, W.A.; Jackson, K.A.; Rutter, J.W.; Chalmers, B. The redistribution of solute atoms during the solidification of metals. *Acta Metall.* **1953**, *1*, 428–437. [CrossRef]
30. Cziegler, A.K.; Schumacher, P. Preliminary Investigation of the Grain Refinement Mechanism in Cu Alloys. In *Shape Casting, Proceeding of the 6th International Symposium (TMS 2016), Nashville, TN, USA, 14–18 February 2016*; John Wiley & Sons, Inc.: Hoboken, NJ, USA, 2016; pp. 159–166.
31. Balart, M.J.; Patel, J.B.; Gao, F.; Fan, Z. Grain refinement of deoxidized copper. *Metall. Mater. Trans. A* **2016**, *47*, 4988–5011. [CrossRef]
32. Cziegler, A.K.; Schumacher, P. Investigation of the correlation between growth restriction and grain size in Cu alloys. *Int. J. Cast Met. Res.* **2017**, *30*, 251–255. [CrossRef]
33. Stefanescu, D.M. Thermal analysis—Theory and applications in metalcasting. *Int. J. Metalcast.* **2015**, *9*, 7–22. [CrossRef]
34. Spittle, J.A.; Sadli, S. Effect of alloy variables on grain refinement of binary aluminium alloys with Al–Ti–B. *Mater. Sci. Technol.* **1995**, *11*, 533–537. [CrossRef]
35. Günther, R.; Hartig, C.; Bormann, R. Grain refinement of AZ31 by (SiC)P: Theoretical calculation and experiment. *Acta Mater.* **2006**, *54*, 5591–5597. [CrossRef]
36. Kurz, W.; Fisher, D.J. *Fundamentals of Solidification*, 4th ed.; Trans. Tech. Publications: Uetikon-Zürich, Switzerland, 1998.
37. Maxwell, I.; Hellawell, A. A simple model for grain refinement during solidification. *Acta Metall.* **1975**, *23*, 229–237. [CrossRef]

38. Quested, T.E.; Greer, A.L. The effect of the size distribution of inoculant particles on as-cast grain size in aluminium alloys. *Acta Mater.* **2004**, *52*, 3859–3868. [CrossRef]
39. Men, H.; Fan, Z. Effects of solute content on grain refinement in an isothermal melt. *Acta Mater.* **2011**, *59*, 2704–2712. [CrossRef]
40. Ejima, T.; Kameda, M. Diffusion of iron and cobalt in liquid copper. *J. Jpn. Inst. Met.* **1969**, *33*, 96–103. [CrossRef]
41. Stefanescu, D.M. *Science and Engineering of Casting Solidification*; Springer: Boston, MA, USA, 2002.
42. Lee, Y.C.; Dahle, A.K.; StJohn, D.H. The role of solute in grain refinement of magnesium. *Metall. Mater. Trans. A* **2000**, *31*, 2895–2906. [CrossRef]
43. Klösch, G. Kornfeinen von Aluminiumhältigen Magnesiumlegierungen. Ph.D. Thesis, Montanuniversitaet Leoben, Leoben, Austria, 2006. (In German)
44. Cziegler, A.K. Aspects of Grain Refinement in Copper Alloys. Master's Thesis, Montanuniversitaet Leoben, Leoben, Austria, 2015.